A Rolling Rig for Propeller Performance Testing

Or D. Dantsker* and Michael S. Selig†
University of Illinois at Urbana–Champaign, Urbana, IL 61801

Renato Mancuso‡
Al Volo LLC, Urbana, IL 61801

A rolling rig for propeller performance testing was developed. The rolling rig presented was used for performance testing of a Mejzlik 27 x 12 TH propeller, which is used on the UIUC AeroTestbed and the UIUC Subscale Sukhoi unmanned research aircraft. The performance parameters measured for the propeller will be used in the future to aid in the calculation of the aerodynamic coefficients of these aircraft. The rolling rig was instrumented to measure flow speed, propeller rotation rate, thrust, torque, air temperature, and air pressure, in order to find the thrust and torque vs. rotation rate curves as well the thrust coefficient, power coefficient, efficiency curves for the propeller. The rig, which is mounted onto a vehicle, was designed and fabricated to be portable such that it is assembled of three sub-assemblies: a platform, a shrouded vertical beam, and a testing apparatus. The rolling rig underwent extensive initial testing including simulated thrust and torque calibration, thermal imaging, and flow visualization. Results for the propeller from experiments performed at flow speeds of 0–60 mph are presented.

Nomenclature

C_P	=	power coefficient
C_T	=	thrust coefficient
D	=	propeller diameter
J	=	advance ratio
n	=	propeller rotation rate
p	=	pressure
Q	=	torque
R	=	universal gas constant
T	=	thrust, temperature
V	=	velocity
η	=	propeller efficiency
ρ	=	density of air

I. Introduction

This paper describes a rolling rig for propeller performance testing. The rolling rig, which is mounted onto a towed-trailer, is designed to measure: flow speed (V), rotation rate (n), thrust (T), and torque (Q), as well as air temperature (T) and pressure (p), in order to find the thrust and torque vs. rotation rate curves as well as thrust coefficient (C_T), power coefficient (C_P), and efficiency (η) vs. advance ratio (J) curves for the propeller. Tests were performed by varying the rotation rate of the propeller while driving over a range of speeds. The rolling rig is adjustable such that the propellers with diameters between 1 and 3 ft can be tested while maintaining a distance of at least 2 diameters away from the vehicle, thereby minimizing interference effects.

*Ph.D. Student, Department of Aerospace Engineering, AIAA Student Member. dantske1@illinois.edu
†Professor, Department of Aerospace Engineering, AIAA Associate Fellow. m-selig@illinois.edu
‡Embedded Systems Engineer. renatomancuso@alvolo.us

Figure 1. The rolling rig on a trailer before road testing.

This paper will present an implementation of the rolling rig for performance testing of Mejzlik 27 x 12 TH propeller, which is used on the UIUC AeroTestbed[1] and the UIUC Subscale Sukhoi[2] unmanned research aircraft. The performance parameters that were measured allowed for the aerodynamic coefficients of these aircraft to be calculated; the aerodynamic forces and moments are found by subtracting the propeller force and moment measured, as well as the gravitational force, from the total forces and moments applied to the aircraft, which are found through measurements from the inertial measurement unit located on the aircraft. The rolling rig is shown in Fig. 1.

This paper will first briefly examine similar road-based platforms used for testing, followed by a description of the design and development of the rig. Next, initial testing results are presented, which includes load cell calibration and flow property characterization. Results from testing the Mejzlik 27 x 12 TH propeller will be presented along with a brief discussion. Finally, a conclusion discussing the results is given.

A. Background

There have been quite a few examples of traditional wind tunnel techniques being performed outside of a wind tunnel. An early example was Tigner et al.,[3] who discussed determining the stability derivatives of an aircraft using a semi-constrained car-top testing technique. More recently, Lundstrom and Amadori[4] used car-top testing to measure the aerodynamic forces and moments of their aircraft and identified dutch rolling tendencies.

Yet, car-top testing has not only been constrained to the testing of aircraft but also to propulsion systems. Cosentino and Murray[5] tested a custom built turbofan using a thrust and torque measuring rig mounted on top of a pickup truck. The rig, which sat in the bed of the pickup truck, anchored the turbine about 1 yard (1 meter) above the roof of the cab and therefore was likely in the wake of the cab. Lundstrom also did car-top testing of a small micro air vehicle propeller.[6] He mounted the testing rig onto a tall roof-rack mounted tripod and thereby placed it well above the slipstream of the car. Moore et al.[7] tested a 5-bladed carbon fiber propeller using a rig mounted on top and in front of the hood of a pickup truck. Moore et al. have also been testing the LEAPTech HEIST, which is a truck-based test rig for testing distributed electric propulsion. Most recently, Chaney et al.[8] tested a 19 in and a 22 in propeller using a rig mounted to a steel frame, holding the rig 22 in (0.56 m) above the roof of a car.

These car-top testing examples point to the importance of placing the testing rig elements well outside the slipstream of the road and the car. A parallel can be drawn to the wind tunnel, where it is said by Deters[9] that a propeller must be at least 1.5 diameters away from a fairing to minimize the effects caused by the fairing. Similar guidelines have been given for distancing the propeller tips from the tunnel walls. These guidelines were used to size the rig presented in this paper.

II. Design and Development

The concept of the rolling rig began due to a lack of performance data for the Mejzlik 27 x 12 TH propeller, used on both the UIUC AeroTestbed[1] and the UIUC Subscale Sukhoi.[2] The importance of attaining propeller performance data follows that in order to find the aerodynamic coefficients while the motor is on, the thrust and torque generated by the propeller must be known at all times. More specifically, the aerodynamic coefficients are calculated from the aerodynamics forces and moments, which are found by subtracting the propeller force and moment, along with the gravitational force, from the total forces and moments applied to the aircraft (these are derived from the inertial measurement unit located on the aircraft).

The rolling rig was designed and fabricated to be portable in that it is assembled of three sub-assemblies: a platform, a shrouded vertical beam, and a testing apparatus. The platform anchors the rig by securing it to the vehicle; the platform is made up of a reinforced wood floor, a square tubing framework, and a reinforced central vertical attachment socket. The vertical beam is a piece of rectangular tubing with adapter blocks that connect to the testing apparatus and the platform; the beam could be fabricated to a variety of lengths to accommodate for propeller sizes. The testing apparatus connects the motor with the load cells that measure torque and moment and holds the energy source as well as all the instrumentation. Both the vertical beam and testing apparatus have fairings to minimize flow disturbance. A CAD rendering of the rolling rig, mounted atop a pickup truck, is shown in Fig. 2. It should be noted that pickup truck shown in the rendering was used during design and build periods, however, due to lack of availability, the rolling rig was placed and towed atop a 4x8 ft no-floor trailer during testing; the trailer configuration mentioned is shown in other figures (i.e., Fig. 1).

The testing apparatus of the rolling rig contains all of the instrumentation needed to measure the flow speed, propeller rotation rates, and motor power. These measurements were performed by an Al Volo FDAQ data acquisition system[10]through a differential pressure sensor-based pitot probe, a motor pulse tachometer, and a current transducer and voltmeter, respectively. Thrust and torque are measured by two 100 kg S-type load cells, which are integrated in to the most forward section of the testing apparatus as shown in Fig. 3, and these are connected to a multi-input Wheatstone bridge interface, which was custom integrated into the same Al Volo data acquisition system. The motor is powered by an electronic speed controller (ESC) that is controlled by a PWM signal from a radio control receiver; the commanding PWM signal is also logged by the same data acquisition system. The Al Volo FDAQ records all data at 400 Hz into internal memory as well as transmitting the data to a laptop running a custom graphical user interface. Specifications of the rolling rig testing apparatus are given in Table 1, and specifications of the propulsion system are given in Table 2.

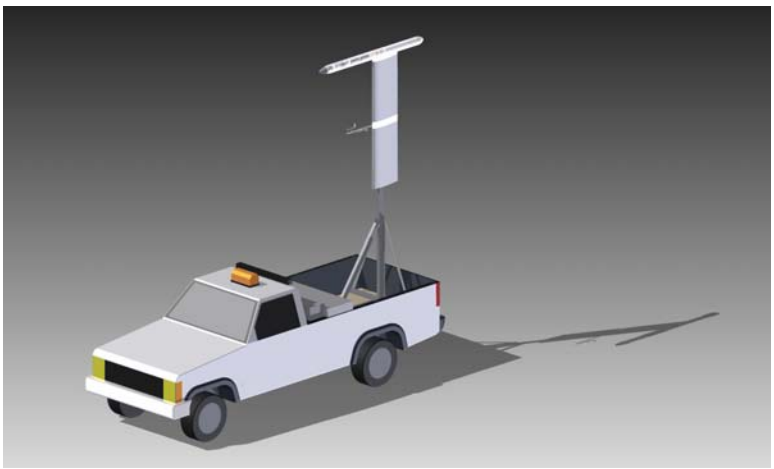

Figure 2. A CAD rendering of the rolling rig mounted on a pickup truck.

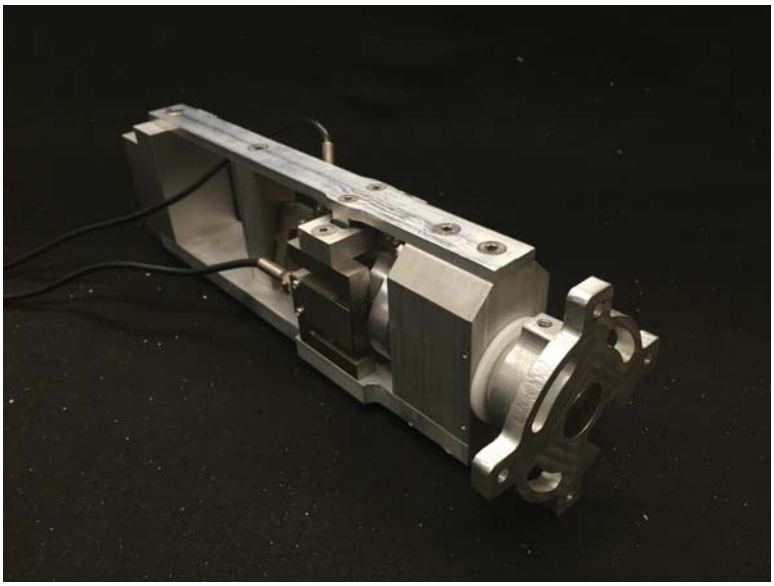

Figure 3. The most forward section of the testing apparatus, designed to decouple and measure thrust and torque, contains two 100 kg S-type load cells.

Table 1. Specifications of the Rolling Rig Testing Apparatus.

Data acquisition system	Al Volo FDAQ 400 Hz system
Inertial and Flow Sensors	
Inertial measurement unit	XSens MTi-G-700 AHRS with GPS
Airspeed probe	EagleTree Systems pitot-static probe
Airspeed sensor	All Sensors 20cmH2O-D1-4V-MINI differential pressure sensor
Wind vanes	2x custom 3D printed at the University of Illinois
Motor Sensors	
Voltmeter	Voltage divider circuit connected to FDAQ analog input
Ammeter	CE-IZ04-35A2-1.0/0-250A DC hall-effect current transducer connected to FDAQ analog input
Tachometer	Custom integration by Al Volo LLC
Load Sensors	
Load Cells	2x CZL301C S-type 100 kg cells
Wheatstone Bridge	Custom integration by Al Volo LLC

Table 2. Specifications of the Tested Propulsion System.

Propeller	Mejzlik 27x12TH
Motor	Hacker A150-8 Outrunner
Electronic Speed Controller	Hacker MasterSPIN 220 Opto
Motor Power Switch	Emcotec SPS 120/240 with RCS PWM Switch
Batteries	(4) Thunder Power ProPerformance 45c 7S 5000 mAh in 2S2P config.

III. Initial Testing

The rolling rig was calibrated and tested before being used to collect data. Specifically, the rolling rig testing apparatus was calibrated for both thrust and torque. Then, the whole system was tested indoors while being thermally imaged. Finally, tufts were placed on the vertical beam fairing to visualize and assess the quality of the flow the testing apparatus experiences.

A. Calibration

The most forward section of the testing apparatus of the rolling rig containing the load cells was calibrated to ensure there was no coupling between the load cell measuring thrust and that measuring torque. The calibration was done using a specifically designed calibration fixture as follows. Simulated thrust was generated by loading the motor mount with s forward force from the left and right mounting points. Simulated torque was generated by loading the motor mount with leftward and rightward forces being applied to the top and bottom mounting points, respectively. The calibration consisted of a cross of 10 forces and 10 torques, each from zero to the 200% of the expected experimental values, totaling 100 combinations. Figures 4 and 5 show the results of the calibration. Along with providing a conversion factor between the load cell outputs and the simulated thrusts and torques applied, the calibration showed that all of the measurements fell within close agreement to the linear trend lines.

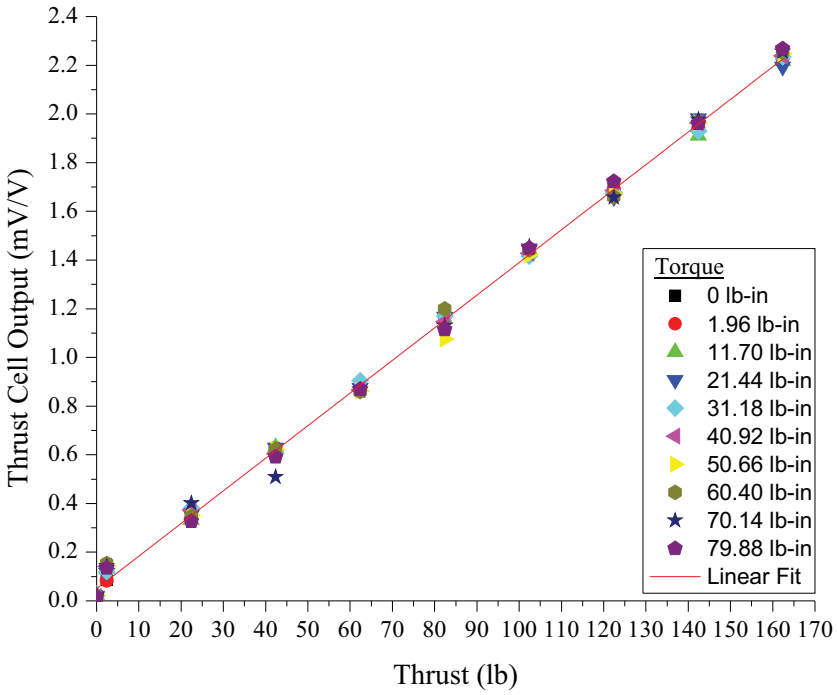

Figure 4. Load cell output vs. thrust for varying torques.

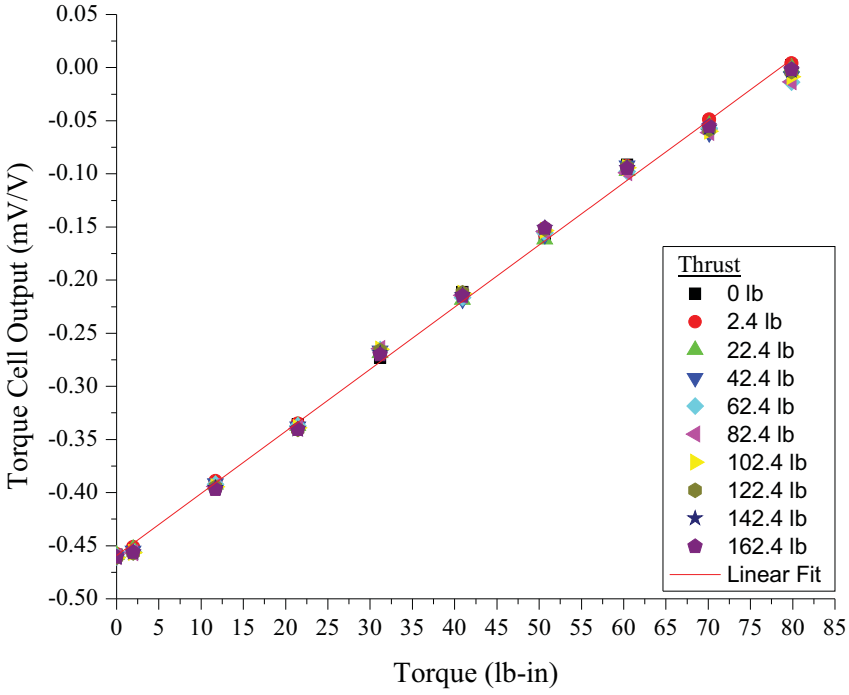

Figure 5. Load cell output vs. torque for varying thrusts.

B. Indoor Testing

The rolling rig was thoroughly tested indoors before performing full-length motor runs. Based on previous experience, it was determined that the shrouds and fairings needed to be removed from the testing apparatus in order to allow for the motor, electronic speed controller, and batteries to properly cool. After everything was removed, the motor was run at varying throttle settings for several minutes. An infrared camera was used to measure the external motor temperature during the test. Near the end of the run, the motor was run to full power for 30 seconds to simulate a worse case temperature, while being continually monitored. A thermal infrared image can be seen in Fig. 6 that shows the rolling rig after 30 seconds of full power testing. As the image shows, by the end of the run, the motor, which is illuminated by the red crosshair, reached a temperature of 61.9°*C*, which is well below the known operating limit of 80°*C*. Therefore, the test was considered a success and testing was allowed to proceed.

Figure 6. A thermal infrared image of the rolling rig motor after 30 seconds of full power.

C. Flow Visualization

In order to assess the quality of flow that the testing apparatus and therefore the propeller experiences, tufts were placed onto the 6 ft tall vertical beam fairing. As can be seen in Fig. 7, the tufts, which were 2.5 in long, were placed in a square grid with 3 in separation. The rig was driven at speeds between 0 and 60 mph, as the rolling rig would be ultimately used within that range of speeds. Figure 8 shows photos of the tuft at speeds of 10, 20, 30, and 40 mph. It should be noted that speeds at and above 40 mph yielded virtually identical tuft behavior.

For the 10 and 20 mph cases, there is an easily discernible angle difference between the tufts below and above the 6th row of tufts from the bottom. In the 30 and 40 mph cases, there seems to a minor amount of a difference in first couple rows from the bottom. Based on what is seen in the photos, it is possible to deduce that the tow vehicle only affects the flow below the bottom quarter of the fairing. Therefore, the rolling rig testing apparatus and the propeller experience clean flow during testing.

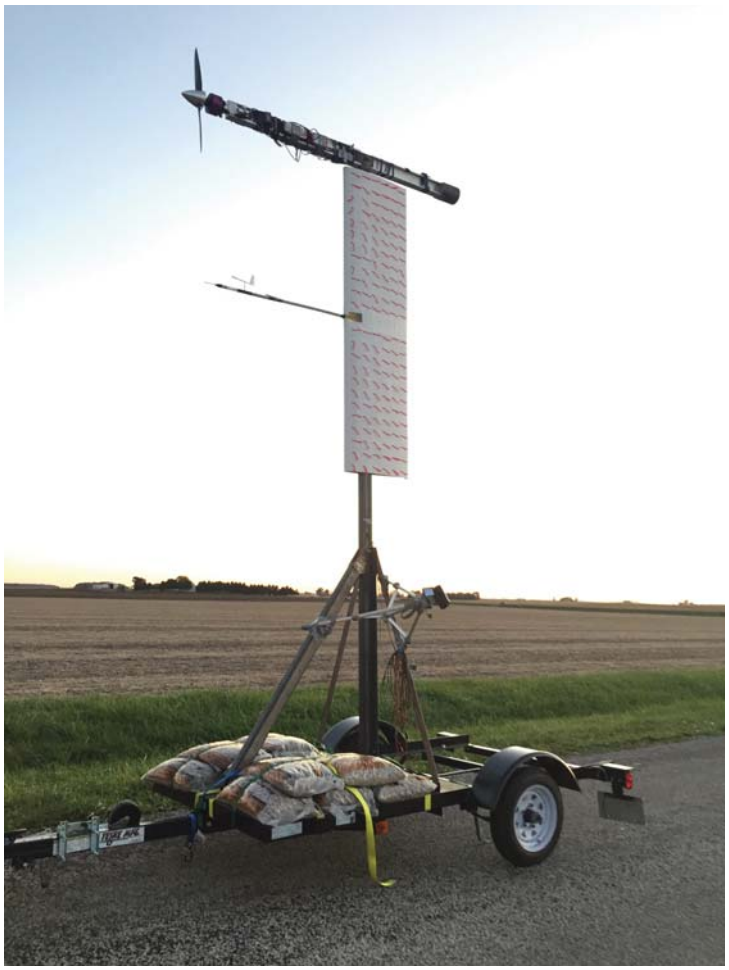

Figure 7. Tufts placed on the vertical beam fairing of the rolling rig to visualize airflow.

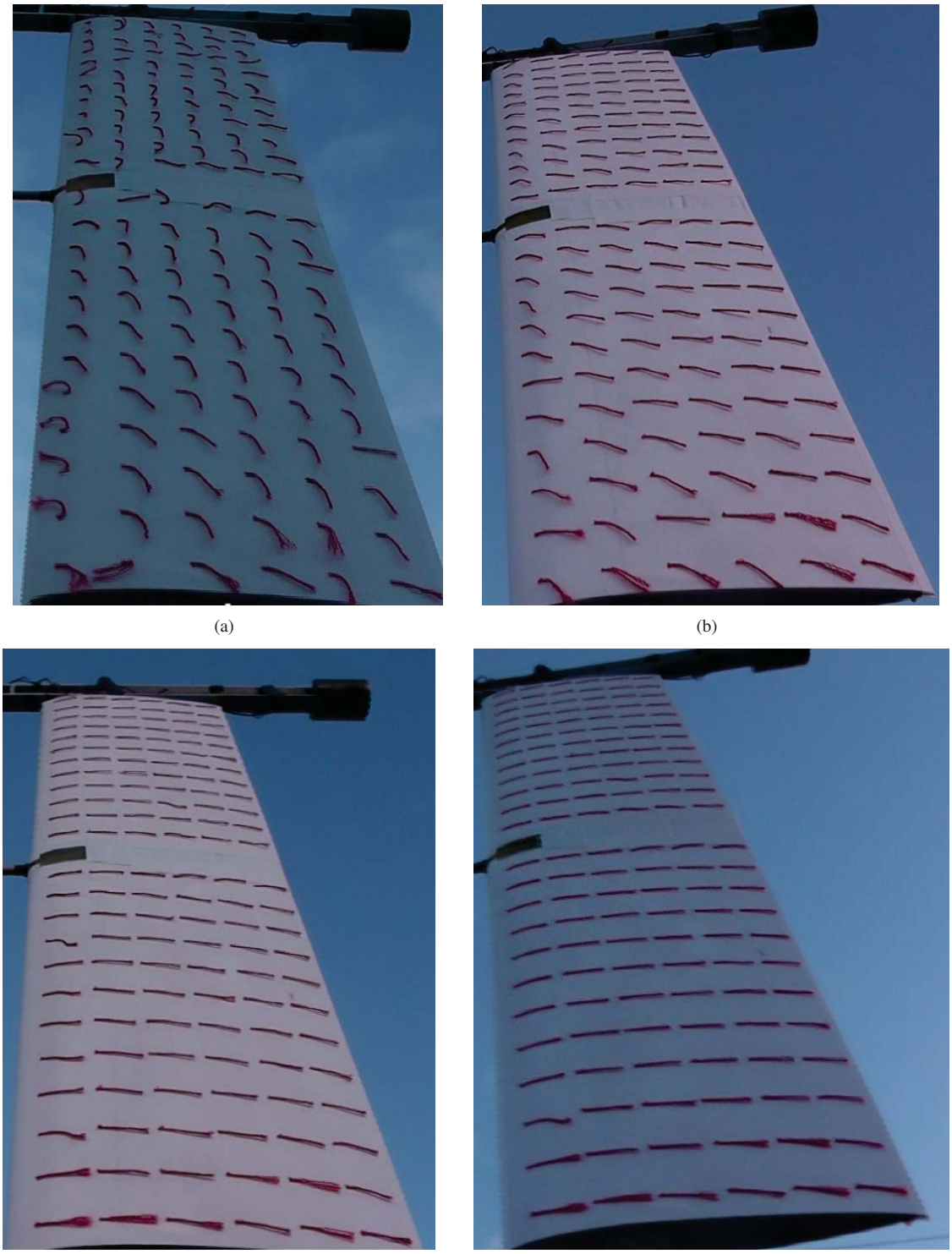

Figure 8. Tufts placed on vertical beam fairing used for flow visualization at (a) 10 mph, (b) 20 mph, (c) 30 mph, and (d) 40 mph.

IV. Data Reduction

When the rolling rig was used for propeller testing, the FDAQ data acquisition system logged raw thrust, torque and rotation rate among other data. Figure 9 shows an example output for the Mejzlik 27 x 12 TH propeller tested statically. There is a large level of noise present in the load and torque measurements, which is likely the result of the vibrations created by the motor and the load cells used. However, averaging the data within the sample ranges of each rotation rate yields a value with an acceptable standard deviation. Additionally, it can also be seen in the figure that rotation rate measurements sometimes oscillate between two or three values, which is the result of how rotation rate is measured. Specifically, the rotation rate was measured by counting the number of motor pulses within a time window. So if the time window is increased, the precision of the measurement is higher but the frequency of measurement is lower. In testing the Mejzlik 27 x 12 TH propeller, the Hacker A150-8 used has 14 poles and the time window was 1/10 sec (10 Hz), so each pulse measured yields 42.8 RPM[†].

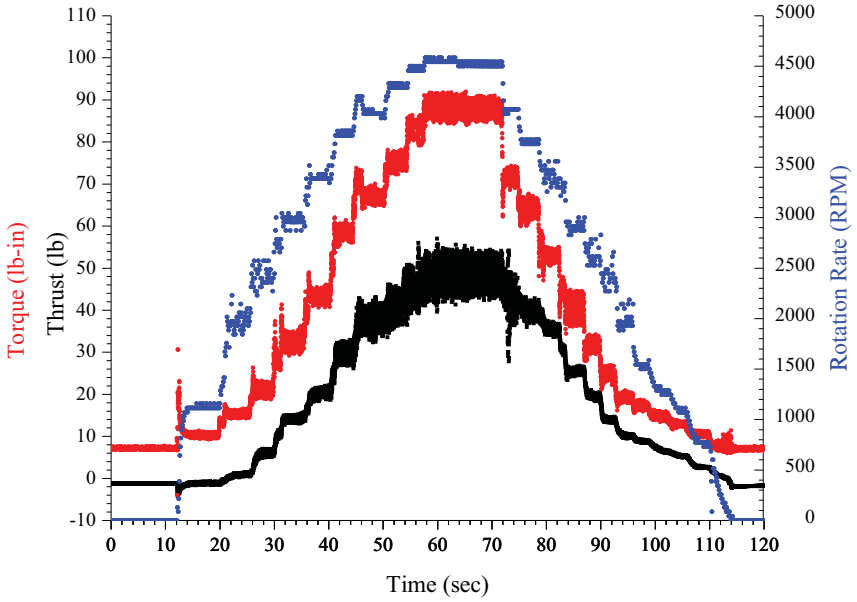

Figure 9. Raw thrust, torque, and rotation rate measurements for the Mejzlik 27 x 12 TH propeller at static conditions.

A script was written to efficiently process the 2.5 million lines of data the FDAQ collected in the 1.5 hours of combined testing. The script allowed the user to quickly select ranges of times when the motor was operating at a stable rotation rate, which would then be averaged to produce thrust, torque, and rotation rate values. The thrust and torque values are also corrected for the drag created by the spinner cone using a static case in each test run as the baseline value.

From the thrust, torque, rotation rate, and flow velocity values, the thrust coefficient, power coefficient, efficiency values are calculated. In order to perform these calculations, knowledge of the air density and propeller diameter is required. Using the temperature and pressure readings, which are also logged by the FDAQ at 400 Hz, the air density is determined using the equation of state

$$p = \rho RT \tag{1}$$

where R is the universal gas constant with a value for air of $1716 \text{ft}^2/\text{s}^2/^\circ\text{R}$ ($287.0 \text{m}^2/\text{s}^2/\text{K}$).

† $\frac{\text{Rotation Rate}}{\text{Pulses Measured}} = \frac{(10 \text{ samples/sec}) \times (60 \text{ sec/min})}{(14 \text{ pulse/rot})} = 42.8$ RPM/pulse, where the number of pulses per rotation is equal to the number of poles the tested motor has.

The propeller advance ratio is defined from the ratio of the measured air flow speed to the propeller rotation rate and the propeller diameter as

$$J = \frac{V}{nD} \tag{2}$$

The thrust coefficient is calculated from the measured thrust, rotation rate, air density, and the propeller diameter as

$$C_T = \frac{T}{\rho n^2 D^4} \tag{3}$$

In order to determine the power coefficient, propeller output power must be found. Propeller power is determined from the measured torque and rotation rate by

$$P = 2\pi n Q \tag{4}$$

Therefore, the power coefficient can be calculated from the measured rotation rate, propeller power, air density, and the propeller diameter as

$$C_P = \frac{P}{\rho n^3 D^5} \tag{5}$$

Finally, the propeller efficiency can be determined as

$$\eta = J\frac{C_T}{C_P} \tag{6}$$

V. Results and Discussion

The rolling rig was used to test the Mejzlik 27 x 12 TH propeller through the full range of rotation rates that the motor used could produce and at speeds of 0, 10, 20, 30, 40, and 60 mph. Figure 10 shows thrust and torque vs rotation rate for the different flow speeds. The values were corrected against for the spinner cone drag. For comparison purposes, thrust and torque values were referenced back to the static run test air density of $0.0021977 \text{slug}/\text{ft}^3$ ($1.1326 \text{kg}/\text{m}^3$).

The thrust and torque data show expected trends; however, the curves are not smooth. The lack of smoothness is the result of the low number of data points collected, due to the logistic difficulty involved in road testing. In addition, the deviations seen in the curves are attributed to the large level of noise that can be seen in the raw sensor output plot. The noise is likely the result of the vibrations created by the motor as well as inertia loads caused by road conditions.

From the flow speed, propeller rotation rate, thrust, torque, air temperature, and air pressure data, curves for the thrust coefficient, power coefficient, and efficiency for the propeller were computed using the data reduction methods presented in Section IV. Figure 11 shows the thrust coefficient, power coefficient, and efficiency curves for the Mejzlik 27 x 12 TH propeller for rotation rates of 4000, 4500, and 5000 RPM. These rotation rates were of interest as they are characteristic of flight conditions and represent a range of values where there is greater confidence in measurement, as compared to lower rotation rates. At higher rotation rates, there were less deviations in the thrust and torque curves, which were the result of a higher number of measurements, due to finer motor control at high rotation rates, and therefore also required less interpolation.

The thrust coefficient, power coefficient, and efficiency figures show expected trends for the low- to mid-range of advance ratios measured. The maximum speed limit of the trailer used in testing prevented data at higher advance ratios from being acquited. It is assumed that at greater advance ratios (i.e., higher testing speeds), the curves in each of the figures would overlap as is typical for propellers. In the case of the efficiency curves in Fig. 11 (c), it can be seen that the propeller has reached its maximum efficiency around the most rightwards data points ($J \approx 0.6$) and expect that measurements taken at larger advance ratios would show decreases in efficiency.

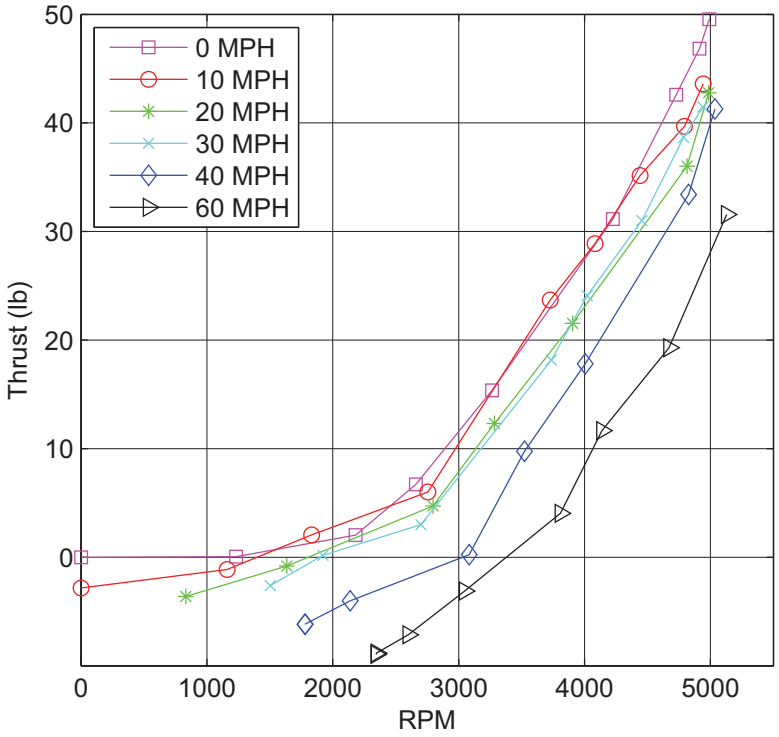

(a)

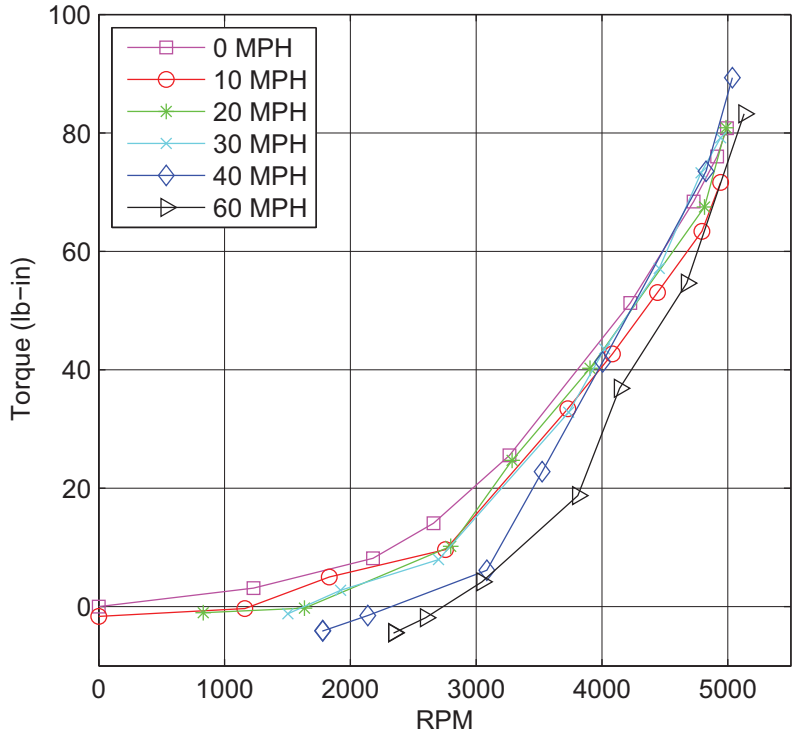

(b)

Figure 10. Thrust (a) and torque (b) vs. rotation rate for the Mejzlik 27 x 12 TH propeller at flow speeds of 0, 10, 20, 30, 40, and 60 mph.

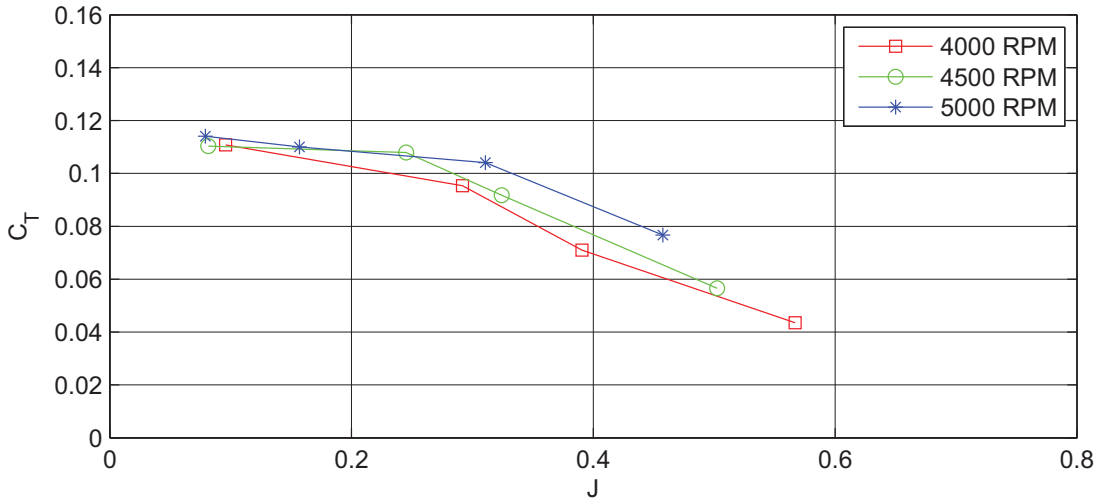

(a)

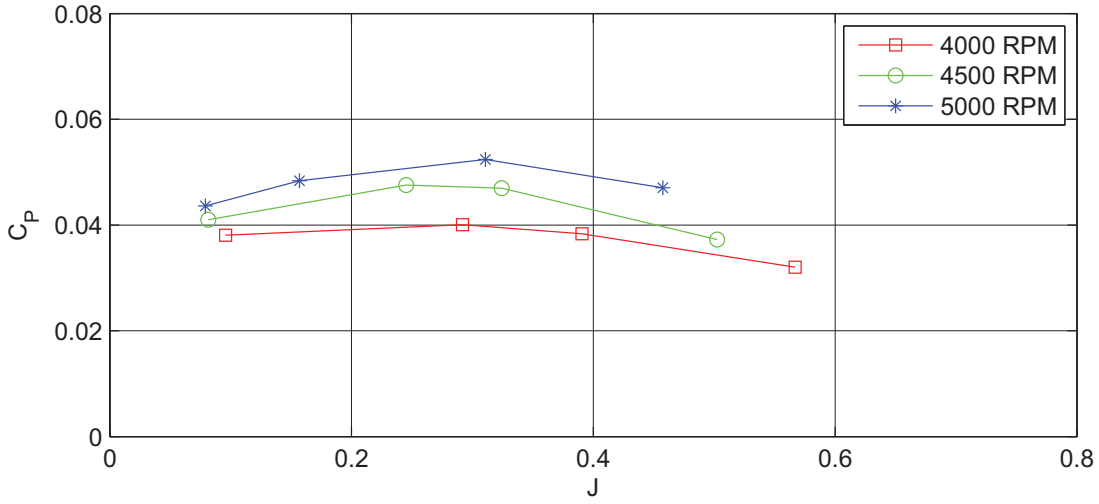

(b)

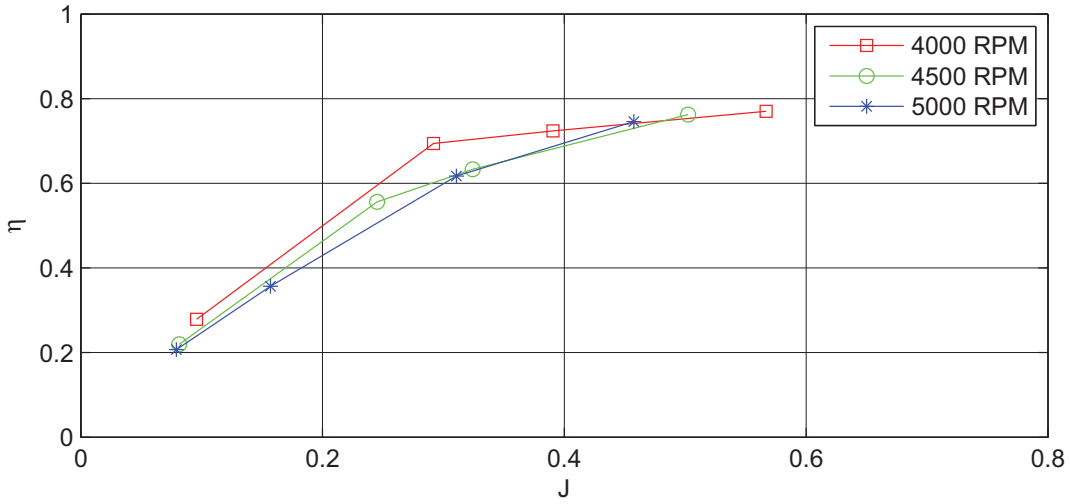

(c)

Figure 11. Performance curves for the Mejzlik 27 x 12 TH propeller at rotation rates of 4000, 4500, and 5000 RPM: (a) thrust coefficient, (b) power coefficient, and (c) efficiency.

VI. Conclusions

A rolling rig was designed and then used for performance testing of a Mejzlik 27 x 12 TH propeller. The rolling rig was instrumented such that it could measure flow speed, rotation rate, thrust, torque, air temperature, and air pressure. The data collected allowed for the thrust and torque vs. rotation rate curves of a propeller to be obtained, which were then reduced to generate thrust coefficient, power coefficient, and efficiency curves of the propeller.

Before the rolling rig was used for propeller performance testing, it underwent extensive initial testing. The initial testing included simulated thrust and torque calibration, which showed that the measurement section of the rig was successfully able to decouple thrust and torque and had linear trends. Then thermal imaging showed that once shrouds and fairings initially included in the design were removed, the motor, electronic speed controller, and batteries were able to safely operate below their maximum temperature limits. Finally, flow visualization of the vertical beam fairing using tufts showed that the propeller is experienced clean flow.

Through experiments, thrust and torque vs. rotation rate curves were obtained for flow speeds of 0, 10, 20, 30, 40, and 60 mph were presented. The data collected was used to calculate thrust coefficient, power coefficient, efficiency curves for the propeller at typical flight condition rotation rates of 4000, 4500, and 5000 RPM. These curves showed trends expected for propellers and in the future will be used for aerodynamic analysis of several unmanned aircraft, which use the Mejzlik 27 x 12 TH propeller. Specifically the data generated will be used to account for the propeller thrust and torque contributions from the total aircraft forces and moments measured by an inertial measurement unit found on the aircraft.

Acknowledgments

We gratefully acknowledge Hoong Chieh Yeong, Ali El-Ashri, Iavor Boykov, Moiz Vahora, Mohammed Qadri, and Shie-Jene Shan for their support during the construction and testing. The authors owe thanks to Al Volo LLC for their generous loan of equipment.

References

[1]Dantsker, O. D., Johnson, M. J., Selig, M. S., and Bretl, T. W., "Development of the UIUC Aero Testbed: A Large-Scale Unmanned Electric Aerobatic Aircraft for Aerodynamics Research," AIAA Paper 2013-2807, AIAA Applied Aerodynamics Conference, San Diego, California, Jun. 2013.

[2]Dantsker, O. D. and Selig, M. S., "High Angle of Attack Flight of a Subscale Aerobatic Aircraft," AIAA Paper 2015-2568, AIAA Applied Aerodynamics Conference, Dallas, Texas, Jun. 2015.

[3]Tigner, B., Meyer, M. J., Holdent, M. E., Rawdon, B. K., Page, M. A., Watson, W., and Kroo, I., "Test Techniques for Small-Scale Research Aircraft," AIAA Paper 98-2726, AIAA Applied Aerodynamics Conference, Dallas, Texas, Jun. 2015.

[4]Lundstrom, D. and Amadori, K., "Raven: A Subscale Radio Controlled Business Jet Demonstrator," In: proceedings from the ICAS 2008, CD-ROM: International Council of the Aeronautical Sciences, Anchorage, Alaska, Sept. 2008.

[5]Cosentino, G. B. and Murray, J. E., "The Design and Testing of a Miniature Turbofan Engine," SAE 2009 Aerotech Congress and Exhibition, Seattle, Washington, Nov. 2009. NASA Report 09ATC-0241, DFRC-1074.

[6]Lundstrom, D. and Krus, P., "Testing of Atmospheric Turbulence Effects on the Performance of Micro Air Vehicles," *International Journal of Micro Air Vehicles*, Vol. 4, No. 2, Jun. 2012, pp. 133–149.

[7]Moore, M., Clarke, S., Stoll, A., Clark, A., MacAfee, S., and Foster, T., "Affordable Flight Testing of LEAPTech Distributed Electric Propulsion," NASA Aeronautics Research Mission Directorate 2015 LEARN/Seedling Technical Seminar, NASA Langley Research Center, Langley, VA, Jan. 2015.

[8]Chaney, C. S., Bahrami, J. K., Gavin, P. A., Shoemake, E. D., Barrow, E. S., and Matveev, K. I., "Car-Top Test Module as a Low-Cost Alternative to Wind Tunnel Testing of UAV Propulsion Systems," *Journal of Aerospace Engineering*, Vol. 27, No. 6, Nov. 2014.

[9]Deters, R. W., *Performance and Slipstream Characteristics of Small-Scale Propellers at Low Reynolds Numbers*, Ph.D. thesis, Dept. of Aerospace Engineering, University of Illinois at Urbana-Champaign, Urbana, IL, Jan. 2014.

[10]Al Volo LLC, "Al Volo: Flight Data Acquisition Systems," http://www.alvolo.us, Accessed Jun. 2017.